Heat capacity and phase equilibria of $KAlSi_3O_8$ hollandite

Wenjun. Yong

Department of Geological Sciences, University of Michigan, Ann Arbor, MI 48109-1005, USA

E-mail: wenjuny@umich.edu

Phone: 001-734-647-5533

Fax: 001-734-763-4690


THE UNIVERSITY OF MICHIGAN
THE UNIVERSITY OF MICHIGAN LIBRARIES

Author

Wenjun Yong

Title

Heat Capacity of $KAlSi_3O_8$ Hollandite and Related Phase Equilibria

submitted in partial fulfillment
of the requirements for the degree of
Master of Science in Geology
Department of Geological Sciences
The University of Michigan

Accepted by:

Signature	Eric J. Essene Name	8/9/2005 Date
Signature	Youxue Zhang Name	8/9/2005 Date
Department Chair	Joel D. Blum Name	8/9/2005 Date

I hereby grant the University of Michigan, its heirs and assigns, the non-exclusive right to reproduce and distribute single copies of my thesis, in whole or in part, in any format. I represent and warrant to the University of Michigan that the thesis is an original work, does not infringe or violate any rights of others, and that I make these grants as the sole owner of the rights to my thesis. I understand that I will not receive royalties for any reproduction of this thesis.

☒ Permission granted.

☐ Permission granted to copy after: _____
Date

☐ Permission declined.

Author Signature

Abstract

The low-temperature isobaric heat capacity (Cp) of $KAlSi_3O_8$ hollandite was measured over the range of 5 – 303 K with a physical properties measurement system (PPMS). The standard entropy of $KAlSi_3O_8$ hollandite is 166.2±0.2 J mol^{-1} K^{-1} , including an 18.7 J mol^{-1} K^{-1} contribution from the configurational entropy due to disorder of Al and Si in the octahedral sites. The entropy of $K_2Si_4O_9$ wadeite was also estimated to facilitate calculation of phase equilibria in the system $KAlSi_3O_8$. The calculated phase equilibria obtained using Perple_x are in general agreement with experimental studies. Phase relations in the system K_2O-Al_2O_3-SiO_2 were also calculated and confirm a substantial stability field for kyanite-stishovite/coesite-$K_2Si_4O_9$ wadeite intervening between $KAlSi_3O_8$ hollandite and sanidine. The upper stability of kyanite is bounded by the reaction $Al_2SiO_5 = Al_2O_3 + SiO_2$ stishovite, which is located at 13-14 GPa for 1100-1400 K. The entropy and enthalpy of formation for $KAlSi_3O_8 \cdot H_2O$ K-cymrite were slightly modified to better fit the Holland and Powell (1998) data base and the previous experimental studies. Thermodynamic calculations were undertaken on the reaction of K-cymrite to $KAlSi_3O_8$ hollandite + H_2O, which is located at 8.3-10.0 GPa for the temperature range 800-1600 K, well inside the stability field of stishovite. The reaction of muscovite to $KAlSi_3O_8$ hollandite + Al_2O_3 + H_2O is placed at 10.0-10.6 GPa for the temperature range 900-1500 K, in reasonable agreement with some but not all experiments on this reaction.

Keywords *Hollandite · Wadeite · K-cymrite · Heat capacity · High-pressure phase equilibria · Thermodynamic calculation*

Introduction

Ringwood et al. (1967) first discovered that potassium feldspar transforms into a hollandite structure when pressure exceeds 12 GPa. The K atoms in $KAlSi_3O_8$ hollandite are accommodated in tunnels formed by double chains of edge-sharing $(Si,Al)O_6$ octahedra (Ringwood et al. 1967; Yamada et al. 1984; Zhang et al. 1993). Kinomura et al. (1975) found an intermediate assemblage of Al_2SiO_5 kyanite, SiO_2 coesite, and $K_2Si_4O_9$ wadeite separating the stability field of sanidine and hollandite. This was verified by additional experiments (Yagi et al. 1994; Urakawa et al. 1994). The lower stability of $KAlSi_3O_8$ hollandite was located to be at pressures of 8-10 GPa for temperatures of 1000-1500 K. With one-fourth of the Si atoms in octahedral sites, the structure of $K_2Si_4O_9$ wadeite can be considered as three-membered rings of SiO_4 tetrahedra connected by octahedrally coordinated Si atoms (Kinomura et al. 1977; Swanson and Prewitt 1983). Liu (1978) reported $KAlSi_3O_8$ hollandite plus a high-pressure form of $KAlO_2$ forming from $KAlSiO_4$ kalsilite in the pressure range of 17-30 GPa. Faust and Knittle (1994) documented the breakdown of a natural muscovite to $KAlSi_3O_8$ hollandite + corundum + H_2O at pressures between 10.9 and 12.0 GPa at around 1073 K. The phase $KAlSi_3O_8$ hollandite has also been reported in hydrated average upper continental crust, MORB, andesite and pelite compositions when pressure is greater than 8 GPa (Irifune et al. 1994; Schmidt 1996; Domanik and Holloway 1996, 2000; Ono 1998; Wang and Takahashi 1999). Electron microprobe analyses of run product hollandite by Domanik and Holloway (2000) show 14-30% deficiencies in the K site that are not matched by excess Si. They inferred that phengite decomposed to $KAlSi_3O_8$ hollandite between 9 and 10 GPa at 900°C. Examination of their assemblages suggests progress of the reaction muscovite + coesite/stishovite = $KAlSi_3O_8$ hollandite + kyanite + fluid, as well as the more complex reactions suggested by the authors that involve magnesite, garnet and OH topaz. The authors noted that their hollandite was damaged by the electron beam but did not correct for elemental migration. The low K site occupancies probably represent an analytical artifact rather than a vacancy substitution. Konzett and Fei (2000) reported $KAlSi_3O_8$ hollandite

as one of the breakdown product at 20-23 GPa and 1773-1973 K in peralkaline and subalkaline rock compositions. Quench experiments by Tutti et al. (2001) showed that $KAlSi_3O_8$ hollandite is still stable even when pressure is as high as 95 GPa, which strongly supports previous suggestions that $KAlSi_3O_8$ hollandite is an important host for potassium in the lower mantle (Ringwood 1975; Prewitt and Downs 1998). Collectively, the experimental studies suggest that $KAlSi_3O_8$ hollandite plays an important role in transporting potassium through the subduction of oceanic crust into the deep mantle. Occurrences of natural $KAlSi_3O_8$ hollandite and $NaAlSi_3O_8$ hollandite have been reported in shocked meteorites (Akaogi 2000; Gillet et al. 2000; Langenhorst and Poirier 2000; Tomioka et al. 2000; Kimura et al. 2004). Sueda et al. (2004) demonstrated that $KAlSi_3O_8$ hollandite transforms to a new high-pressure phase (hollandite II) at ~22 GPa at room temperature using in situ X-ray diffraction. They related this transition to the changes in both composition and melting observed in experiments on $KAlSi_3O_8$ hollandite wih 3-15 mol% $CaAl_2Si_2O_8$ and 9-18 mol% $NaAlSi_3O_8$ in a basaltic system by Wang and Takahashi (1999).

The thermodynamic properties of several phases are in need of further study in order to accurately determine the phase equilibria in the system K_2O-Al_2O_3-SiO_2, although some measurements have been made. The enthalpy of $K_2Si_4O_9$ wadeite and $KAlSi_3O_8$ hollandite was measured by Geisinger et al. (1987) and Akaogi et al. (2004). The high-temperature heat capacity of $K_2Si_4O_9$ wadeite was measured by Fasshauer et al. (1998). They generated an internally consistent thermodynamic data set for several phases but did not include $KAlSi_3O_8$ hollandite in their evaluation. Akaogi et al. (2004) measured the high-temperature heat capacity data of $KAlSi_3O_8$ hollandite and reevaluated the phase relations in the system $KAlSi_3O_8$ by combining thermodynamic with experimental data. However, an approach totally independent of the experiments has not been applied to this system because the lack of low-temperature heat capacity data, and hence lack of entropy and Gibbs free energy, of the high-pressure phases. In this study, the low-temperature heat capacity of $KAlSi_3O_8$ hollandite was measured using a physical properties measurement system (PPMS, produced by Quantum Design®), and the

entropy of $KAlSi_3O_8$ hollandite was calculated from the measured heat capacity data. The entropy of $K_2Si_4O_9$ wadeite was estimated from Holland (1989), and phase relations in the system K_2O-Al_2O_3-SiO_2 were calculated based on the new thermodynamic data. Several reactions involving $KAlSi_3O_8$ hollandite were also investigated in the system K_2O-Al_2O_3-SiO_2-H_2O.

Experimental Procedures

Sample synthesis and characterization

The phase $KAlSi_3O_8$ hollandite was synthesized using a 1000-ton Walker-type multi-anvil device at the University of Minnesota. Tungsten carbide anvils with 8 mm truncations, cast MgO- Cr_2O_3 octahedra with 14 mm edge lengths and pyrophyllite gaskets were used for this study. Powdered $KAlSi_3O_8$ glass from Craig Manning at UCLA was used as the starting material, which was powdered and put into a cylindrical Re capsule/furnace and held at 11 GPa and 1273 K for 24 hours, then quenched at 11 GPa and slowly recovered to ambient pressure. Temperature was controlled by $W_3Re_{97}/W_{25}Re_{75}$ thermocouple oriented axially with respect to the heater.

The run product was confirmed to be $KAlSi_3O_8$ hollandite by X-ray diffraction and a electron microprobe analyzer (EMPA). A Scintag X-ray diffractometer was used to obtain the X-ray diffraction pattern of the synthetic $KAlSi_3O_8$ hollandite, from which the lattice parameters were determined using the Scintag program Crystallography; the results are shown in Table 1. The lattice parameters from this study are in good agreement with those of Zhang et al. (1993) and deviate slightly from data of Yamada et al. (1984) (Table 1). The EMPA was undertaken on a Cameca SX-100, and the result is shown in Table 2. The column conditions were: accelerationg voltage 15 kV, beam current 4 nA, peak and background counting times each 30 s, beam scan area 5×5 μm. The standards used for Na, Mg, Al, Fe, Si and K were Tiburon albite, synthetic $MgTiO_3$, fluortopaz from Topaz Mtns., Utah, synthetic $FeSiO_3$, K-feldspar from St.

Gotthard, respectively. Compared to previous EMPA studies on synthetic $KAlSi_3O_8$ hollandite that indicated an apparent deficiency on the K site (Irifune et al. 1994; Schmidt 1996; Domanik and Holloway 1996, 2000; Ono 1998; Wang and Takahashi 1999), the EMPA analysis in this study shows no evidence for a vacancy on that site. Less acurate TEM analyses of natural hollandite structures from shock metamorphosed meteorites also indicated vacancy on the K site, although Ca substitution has certain compensation (Langenhorst and Poirier 2000).

Tables 1, 2

Heat capacity measurement

The low-temperature heat capacity at constant pressure (Cp) of $KAlSi_3O_8$ hollandite was measured at 1 atm using the heat capacity option of the PPMS at Salzburg University in Austria. Based on heat-pulse calorimetry (HPC), the PPMS is the first commercially available apparatus that can measure the low-temperature heat capacity of samples with milligram mass. A 17.91 mg powdered sample of $KAlSi_3O_8$ hollandite was sealed into little flat Al pans with lids and placed on a 4×4 mm wide sapphire platform for heat capacity measurement. The measurement was performed on heating up from 5 K to 303 K with 50 data points. A detailed description of the heat capacity measurements by PPMS and the expected errors is given in Dachs and Bertoldi (2005) and Dachs and Geiger (2005).

Results

Heat capacity and entropy of $KAlSi_3O_8$ hollandite

The measured molar heat capacity (Cp) of $KAlSi_3O_8$ hollandite versus temperature is shown in Table 3 and Fig. 1. To obtain the entropy of $KAlSi_3O_8$ hollandite, a general polynomial form of $Cp = k_0 + k_1T^{-0.5} + k_2T^{-2} + k_3T^{-3} + k_4T + k_5T^2 + k_6T^3$ was chosen to fit the Cp data in Table 3 using the Experimental Data Analyst Package of Mathematica®. The data were split into three temperature regions and each region was fitted individually with some overlap of data. The

equation $Cp = k_0 + k_1T^{-0.5} + k_2T^{-2} + k_3T^{-3}$ was used for fitting the high temperature portion of the data, the complete polynomial given above for the intermediate temperature portion and $Cp = k_4T + k_6T^3$ is for fitting at low temperature. The Cp data below 5 K were estimated by a linear extrapolation to 0 K from the lowest measured Cp point in the form of $Cp = k_6T^3$. The uncertainty in the entropy at STP was estimated by a Monte Carlo technique. A detailed description of error estimation is provided in Dachs and Bertoldi (2005) and Dachs and Geiger (submitted). The entropy of $KAlSi_3O_8$ hollandite at 298.15 K calculated by integration of these fitted functions is 147.5±0.2 J mol^{-1} K^{-1} (error is one standard deviations). Crystal structure refinement of $KAlSi_3O_8$ hollandite shows that Al atoms and Si atoms are fully disordered over the octahedral sites (Yamada et al. 1984; Zhang et al. 1993), thus requiring addition of the configurational entropy into the entropy term obtained by integration. The configurational entropy is calculated from $S_0^\circ = -4R(0.25\ln0.25+0.75\ln0.75) = 18.7$ J mol^{-1} K^{-1}. Including this contribution, the entropy obtained for $KAlSi_3O_8$ hollandite at STP is 166.2±0.2 J mol^{-1} K^{-1}. The results of this study are remarkably larger than the value of 65.3 J mol^{-1} K^{-1} that was estimated by Domanik and Holloway (2000). Their estimate was derived by summation techniques based on a complex dehydration reaction involving phengite in the system KMASH and is likely to have large errors that were not evaluated.

The high-temperature Cp data of $KAlSi_3O_8$ hollandite were measured by Akaogi et al. (2004). Their data were used for calculation of the enthalpy and entropy at high temperatures(Table 4).

Table 3
Figure 1

Entropy of $K_2Si_4O_9$ wadeite and phase equilibria in $KAlSi_3O_8$ system

High-pressure experimental studies on the phase transitions in $KAlSi_3O_8$ were carried out by Yagi et al. (1994) and Urakawa et al. (1994) on the following reactions:

$$2KAlSi_3O_8\ (san) = K_2Si_4O_9\ (wd) + Al_2SiO_5\ (ky) + SiO_2\ (coe) \qquad (1)$$

$$K_2Si_4O_9 \text{ (wd)} + Al_2SiO_5 \text{ (ky)} + SiO_2 \text{ (coe)} = 2KAlSi_3O_8 \text{ (hol)} \qquad (2)$$

$$K_2Si_4O_9 \text{ (wd)} + Al_2SiO_5 \text{ (ky)} + SiO_2 \text{ (stv)} = 2KAlSi_3O_8 \text{ (hol)} \qquad (3)$$

The experimental results are shown in Fig. 2. The quenched experiments by Yagi et al. (1994) were revised based on pressure recalibration (Akaogi et al. 2004), and then are comparable to the in situ X-ray experiments of Urakawa et al. (1994), which were based on a NaCl pressure scale.

Thermodynamic calculations of these equilibria were undertaken with the computer program Perple_x (Connolly and Kerrick 1987; Connolly 1990) using a modified Holland and Powell (1998) data base, and including the new data from this research for $KAlSi_3O_8$ hollandite and $K_2Si_4O_9$ wadeite. Table 4 shows the sources of phase properties involved in this study. For the solid phases, the temperature dependence of the molor volume, V°(T), is given by

$$V^\circ(T) = V^\circ_{298}\left(1 + \int_{298}^{T} \alpha dT\right) \qquad (4)$$

where α and V°_{298} are the thermal expansion and molar volume at standard state, respectively. The pressure dependence of molor volume was calculated using the Murnaghan equation of state:

$$V(T,P) = V^\circ(T)\left(1 + \frac{K'_{0T}}{K_{0T}}P\right)^{-\frac{1}{K'_{0T}}} \qquad (5)$$

where K_{0T} and K'_{0T} are the isothermal bulk modulus and its pressure derivative, respectively. The compensated-Redilich-Kwong (CORK) equation from Holland and Powell (1991, 1998) was chosen for the state of equation of H_2O.

Table 4

Unfortunately, the entropy of $K_2Si_4O_9$ wadeite has not been determined calorimetrically. Fasshauer et al. (1998) estimated a value of 232±10 J mol^{-1} K^{-1} for S°_{298} of $K_2Si_4O_9$ wadeite, about 33 J mol^{-1} K^{-1} larger than that calculated by Geisinger et al. (1987) from spectroscopic data. This is partly supported by the systematically higher Cp observed by differential scanning

calorimetry (DSC) at T < 500 K than that derived from vibrational spectroscopy (Fasshauer et al., 1998). Thermodynamic calculation using Perple_x also favors a larger value for S°_{298} of $K_2Si_4O_9$ wadeite. The calculated phase relations using $S^{\circ}_{298\,(wad)} = 232 \pm 10$ J mol^{-1} K^{-1} are shown in Fig. 2 (dashed lines). Unfortunately, large discrepancies remain between the calculated phase boundaries and the experimental data of Yagi et al. (1994) and Urakawa et al. (1994). An even larger value for S°_{298} of $K_2Si_4O_9$ wadeite is needed to better fit the experimental data with thermodynamic calculations.

To address this problem, the S°_{298} of $K_2Si_4O_9$ wadeite was estimated from Holland (1989) as follows:

$$\begin{aligned} S^{\circ}_{298(wad)} &= (3S^{[4]}_{SiO_2} + S^{[6]}_{SiO_2} + S_{K_2O(a)}) + k[V^{\circ}_{298(wad)} - (3V^{[4]}_{SiO_2} + V^{[6]}_{SiO_2} + V_{K_2O(a)})] \\ &= kV^{\circ}_{298(wad)} + 3(S - kV)^{[4]}_{SiO_2} + (S - kV)^{[6]}_{SiO_2} + (S - kV)_{K_2O(a)} \\ &= 108.44 + 3 \times 17.45 + 10.49 + 79.55 = 250.83 \pm 3 \text{ J mol}^{-1} \text{ K}^{-1} \end{aligned}$$

where k = 1.0 J K^{-1} cm^{-3}, which corresponds to solid-solid reactions involving no change in coordination state that have dP/dT = 10 bar K^{-1}.Because there is no $(S–kV)^{[6]}_{SiO_2}$ in Holland (1989), it was calculated using stishovite data from Holland and Powell (1998) data base. The phase boundary of reaction (1) calculated with the estimated entropy of $K_2Si_4O_9$ wadeite works reasonably well in terms of fitting the experimental data of Yagi et al. (1994) and Urakawa et al. (1994) (solid line in Fig. 2). A small modification that is within the error of $\Delta H^{\circ}_{f,298}$ of $KAlSi_3O_8$ hollandite was applied to make the calculated phase boundaries of reaction (2) and (3) consistent with the experimental data of Yagi et al. (1994) and Urakawa et al. (1994) (solid line in Fig. 2). The calculated boundary for the decomposition of sanidine into kyanite, coesite, and $K_2Si_4O_9$ wadeite in Fig. 2 is almost identical to that determined by Akaogi et al. (2004), and reasonable consistency is obtained with the experimental results of Yagi et al. (1994) and Urakawa et al. (1994) above 1100 K. The difference between the experimental data and the calculated phase boundary below 1100 K can be explained either by sluggish reaction rates or by remaining uncertainties in the thermodynamic properties (Akaogi et al. 2004). The formation of $KAlSi_3O_8$

hollandite by reaction (2) and (3) happens to intersect the coesite – stishovite transition boundary as shown in Fig. 2. The calculated locus of reactions (2) and (3) is 0.3 – 0.4 GPa higher than that of Akaogi et al. (2004). The difference may result from uncertainties in entropy, volume and enthalpy data of $K_2Si_4O_9$ wadeite and $KAlSi_3O_8$ hollandite as well as other thermodynamic properties of all the phases involved in this system. Choosing 8.7 GPa at 1273 K for the phase boundary from Akaogi et al. (2004) might also be a source of the difference. Nonetheless, the result of this study and that of Akaogi et al. (2004) are consistent with the experimental study of Yagi et al. (1994) and Urakawa et al. (1994) within expected errors.

Figure 2

Phase equilibria in K_2O-Al_2O_3-SiO_2

Using the refined values of entropy and enthalpy data of $K_2Si_4O_9$ wadeite and $KAlSi_3O_8$ hollandite as well as the modified Holland and Powell (1998) data base, a P-T diagram for the system K_2O-Al_2O_3-SiO_2 was calculated with Perple_x (Fig. 3). Fasshauer et al. (1998) suggested that sanidine would disproportionate first to $KAlSiO_4$ kalsilite + SiO_2 coesite at around 5 GPa when temperature is above 823 K, and this assemblage would remain stable until pressure reaches 6-7 GPa. However, the calculated P-T diagram doesn't include a region where reaction (1) becomes metastable. The reaction $KAlSiO_4$ kalsilite + $KAlSi_3O_8$ feldspar = Al_2SiO_5 kyanite + $K_2Si_4O_9$ wadeite has been identified both by Fasshauer et al. (1998) and in this study, although the location of the boundary varies somewhat between the two works. For reactions with $K_2Si_4O_9$ wadeite, discrepancies between this study and Fasshauer et al. (1998) are mainly caused by different values of S°_{298} for $K_2Si_4O_9$ wadeite. A calorimetric determination of S°_{298} of $K_2Si_4O_9$ wadeite will be necessary to resolve remaining discrepancies in this system. Several reactions involving Al_2O_3 corundum that Fasshauer et al. (1998) didn't include in their study have also been identified and located provisionally. The reaction kyanite = corundum + stishovite is located at about 13-14 GPa at 1100-1400 K and represents the upper stability of kyanite. The

calculated phase boundary is 0.1-0.2 GPa lower than the experimental results of Schmidt et al. (1997) (Fig. 3, triangles) at temperatures above 1500 K. The disagreement may result from difficulties in extrapolating the Cp data of stishovite to such high temperatures, or relate to possible errors in the pressure calibration of the multi-anvil apparatus.

Figure 3

Phase equilibria in K_2O-Al_2O_3-SiO_2-H_2O

At high water pressures, K-feldspar reacts to form a hydrated phase $KAlSi_3O_8 \cdot H_2O$, called "K-cymrite" (Massonne, 1992) or "sanidine hydrate" (Tompson et al. 1998). A detailed crystal structure study of $KAlSi_3O_8 \cdot H_2O$ by Fasshauer et al. (1997) suggests that it is indeed isostructural with $BaAl_2Si_2O_8 \cdot H_2O$ cymrite, although the Al and Si atoms are highly disordered in $KAlSi_3O_8 \cdot H_2O$ whereas in cymrite the Al and Si atoms are ordered. In this study the informal name K-cymrite will be used for the synthetic phase $KAlSi_3O_8 \cdot H_2O$. Synthesis experiments by Seki and Kennedy (1964) located the phase boundary of following reaction at around 1.8 – 2.8 GPa and 700 – 1000 K.

$$KAlSi_3O_8 \text{ sanidine} + H_2O = KAlSi_3O_8 \cdot H_2O \text{ K-cymrite} \qquad (6)$$

However, experiments by Massonne (1992) on reaction (6) yielded a much flatter phase boundary at around 2.5 GPa, and this result was confirmed by reversed experiments of Fasshauer et al. (1997) and Thompson et al. (1994, 1998). Fasshauer et al. (1997) also adopted a Bayesian method to evaluate the thermodynamic properties of the phases in reaction (6) and derived the standard enthalpy of formation and entropy for K-cymrite. They treated the order-disorder relations of microcline to sanidine with a Landau formalism following Carpenter and Salje (1994). They also noted in a footnote that their STP enthalpy of K-cymrite would have to be changed by –7 kJ/mol to bring the enthalpy of microcline into accord with the revised data of Robie and Hemingway (1995). We recalculated the entropy and enthalpy of formation for K-cymrite to best fit the experimental reversals by Fasshauer et al. (1997) and Thompson et al.

(1998). The revised data are shown in Table 4 and the best fit phase boundary is shown in Fig. 4. The revised enthalpy of formation and entropy for K-cymrite are ~5 kJ mol^{-1} more negative and ~8 J mol^{-1} K^{-1} more positive than the respective values of Fasshauer et al. (1997). The enthalpy shows a +2 kJ/mol disagreement with the revised value of Fasshauer et al. (1997), a relatively small error for such a calculation. The cause of the discrepancy in the estimated entropy of K-cymrite between their study and this work is unclear, because their compressibility and thermal expansion data for K-cymrite were used in the present calculations. The calculated phase boundary for reaction (6) with the revised values of this study are in agreement with experimental reversals of Fasshauer et al. (1997) and Thompson et al. (1998). The calculated phase boundary is located at less than 3 GPa at $T < 1100$ K. Even when a_{H_2O} is as low as 0.5, the pressure needed for the formation of K-cymrite (less than 3.5 GPa: Fig. 4) is less than the peak metamorphic pressure of some UHPM rocks (e.g. Schertl et al. 1991; Sharp et al. 1993; Kaneko et al. 2000; Chopin 2003; Yoshida et al. 2004). Therefore, it is possible that sanidine will hydrate to form K-cymrite during UHPM. However, the occurrence of K-cymrite has not been reported in nature. Hwang et al. (2004) discovered a new polymorph of K-feldspar, kokchetavite, in the well-established ultrahigh-pressure terrane Kokchetav, Kazahkstan. Reminiscent of the experiment by Thompson et al. (1998) who reported a hexagonal $KAlSi_3O_8$ phase (probably isostructural to kokchetavite) when K-cymrite is dehydrated at $T > 1273$ K and at ambient pressure, Hwang et al. (2004) suggested that kokchetavite could represent the dehydration product of K-cymrite during exhumation. Massonne and Nasdala (2003) also described inclusions in garnets made up of quartz, K-feldspar and micaceous materious that possibly formed as pseudomorphs after K-cymrite from a diamondiferous quartzofeldspathetic rock from Erzgebirge, Germany. However, K-cymrite has not been detected directly in the UHP rocks from Erzgebirge and Kokchetav (Massonne and Nasdala 2003; Korsakov et al. 2004). K-cymrite probably dehydrates rapidly to sanidine during exhumation of potassian UHP rocks, especially those that attained relatively high temperature (973-1173 K).

Figure 4

Harlow and Davies (2004) infered a negative P/T slope for the breakdown of K-cymrite based on two experimental runs: 9 GPa at 1473 K and 8 GPa at 1523 K for the reaction

$$KAlSi_3O_8 \cdot H_2O \text{ K-cymrite} = KAlSi_3O_8 \text{ hollandite} + H_2O \quad (7)$$

However, the calculated phase transition boundary shows a slight positive P/T slope and lies 0.4-1.4 GPa higher than the two experimental runs by Harlow and Davies (2004) (Fig. 5). Further calorimetric study of K-cymrite is required to address this discrepancy, and additional work needs to be done to better constrain the phase transition boundary of reaction (7).

Figure 5

Faust and Knittle (1994) documented the breakdown of a natural muscovite, $KAl_3Si_3O_{10}(OH)_2$, to $KAlSi_3O_8$ hollandite at pressures between 10.9 and 12 GPa around 1073 K via the following reaction:

$$KAl_3Si_3O_{10}(OH)_2 = KAlSi_3O_8 \text{ hollandite} + Al_2O_3 + H_2O \quad (8)$$

The upper baric stability of muscovite is controlled by this reaction. Fig. 6 shows the calculated phase transition boundary of reaction (8) using Perple_x and the thermodynamic data in Table 4. The pressure of the calculated phase transition boundary is about 10.1 GPa at temperature of 1073 K and increases to 10.5 GPa at temperature of 1600 K, ~1-2 GPa lower than the experimental results by Faust and Knittle (1994). Considering the large uncertainties of the pressure in the laser-heated diamond cell experiments by Faust and Knittle (1994), the calculated phase boundary is considered to be in general agreement with their experimental results. However, the calculated curve has a considerably different slope than the calculated phase boundary by Sekine et al. (1991) (dashed line in Fig. 6), probably because the phase transition boundaries of reaction (1) and (3) that were used to extrapolate the thermodynamic data of $KAlSi_3O_8$ hollandite were not well constrained at that time.

Figure 6

Sekine et al. (1991) and Faust and Knittle (1994) reported two other dehydration reactions of muscovite:

$$KAl_3Si_3O_{10}(OH)_2 = KAlSi_3O_8 \cdot H_2O \text{ K-cymrite} + Al_2O_3 \qquad (9)$$

$$2KAl_3Si_3O_{10}(OH)_2 = K_2Si_4O_9 \text{ wadeite} + 2Al_2SiO_5 \text{ kyanite} + Al_2O_3 + 2\,H_2O \qquad (10)$$

These two reactions are thought to occur at low pressures. However, the present thermodynamic calculations show that reaction (9) only proceeds above 1700 K, and reaction (10) is a metastable reaction, which requires pressures higher than ~11 GPa, where muscovite has already dehydrated into $KAlSi_3O_8$ hollandite + Al_2O_3 + H_2O.

Discussion

The calculated phase transition boundaries of reaction (2) and (3) constrains the lower stability field of $KAlSi_3O_8$ hollandite at 9-10 GPa for T > 1000 K. Occurrence of $KAlSi_3O_8$ hollandite with stishovite in melt veins of the shocked meteorite Zagami (Langenhorst and Poirier 2000) supports this calculation. Although Tutti et al. (2001) showed that the stability field of $KAlSi_3O_8$ hollandite can attain 95 GPa, representing 2200 km in the mantle, a study by Sueda et al (2004) put the upper stability of $KAlSi_3O_8$ hollandite at 22-24 GPa, where it transforms to a new phase, hollandite II. That is consistent with the crystallization pressure of $KAlSi_3O_8$ hollandite in a shocked meteorite that was estimated to be less than 25 GPa (Langenhorst and Poirier 2000). The locations of reaction (7) and (8) also confirm that $KAlSi_3O_8$ hollandite is stable at pressure above 10 GPa. Based on these studies, it is concluded that $KAlSi_3O_8$ hollandite is an important K-bearing mineral down to depths of 400-660 km in the transition zone of the Earth's mantle and that hollandite II is important at greater depths.

Besides occurrences in shocked meteorites, $KAlSi_3O_8$ hollandite has also been reported as an experimental run product between 8 and 11 GPa in bulk compositions corresponding to average continental crust, subducted sediment, basalt, and metapelite (Irifune et al. 1994; Domanik and Holloway 1996, 2000; Schmidt 1996; Ono 1998; Wang and Takahashi 1999).

However, $K_2Si_4O_9$ wadeite has not yet been identified in any of these experiments or in natural occurrences. Wang and Takahashi (1999) argued that K isselectively partitioned into pyroxene and/or garnet in potassic basalt and would inhibit the formation of $K_2Si_4O_9$ wadeite in that bulk compostion. At high partial pressure of water, reaction (6) will take place at much lower pressure than reaction (1), which also prevent the formation of $K_2Si_4O_9$ wadeite from $KAlSi_3O_8$ sanidine.

Acknowledgments

The authors are grateful to Craig Manning of UCLA for providing 2 g of sanidine glass for use in this study. They also thank Zeb Page and Carl Henderson for their help in EMPA analysis, and Roland C. Rouse for his help with XRD measurements. Edgar Dachs and Anthony Withers are especially appreciated for their experimental contributions. This work was partly supported by Scott Turner Research Grant by the Department of Geological Sciences, University of Michigan to the senior author, and by NSF grants 96-28196, 99-11352 and 00-87448 to EJE. Grants 03-10142 and 00-79827 to M. Hirschmann for the multianvil device at the University of Minnesota, and support of the Austrian granting agency for the PPMS at the University of Salzburg (grant P15880-N11) are also gratefully acknowledged.

References

Akaogi M (2000) Clues from a shocked meteorite. Science 287:1602–1603.

Akaogi M, Kamii N, Kishi A, Kojitani, H (2004) Calorimetric study on high–pressure transitions in $KAlSi_3O_8$. Phys Chem Minerals 31:85–91.

Chopin C (2003) Ultrahigh-pressure metamorphic: tracing continental crust into the mantle. Earth Planet Sci Lett 212:1–14.

Connolly JAD (1990) Multivariable phase diagrams: an algorithm based on generalized thermodynamics. Am J Sci 290:666-718.

Connolly JAD, Kerrick DM (1987) An algorithm and computer program for calculating composition phase diagrams. CALPHAD 11:1–55.

Dachs E, Bertoldi C (2005) Precision and accuracy of the heat–pulse calorimetric technique: low temperature heat capacities of milligram–sized synthetic mineral samples. Eur J Mineral 17:251–259.

Dachs E, Geiger CA (2005) Heat capacities and vibrational entropies of mixing of pyrope-grossular ($Mg_3Al_2Si_3O_{12}$-$Ca_3Al_2Si_3O_{12}$) garnet solid solutions: a low temperature calorimetric and thermodynamic investigation. Am Mineral, in submission

Domanik KJ, Holloway JR (1996) The stability and composition of phengitic muscovite and associated phases from 5.5 to 11 GPa: implications for deeply subducted sediments. Geochim Cosmochim Acta 60:4133–4150.

Domanik KJ, Holloway JR (2000) Experimental synthesis and phase relations of phengitic muscovite from 6.5 to 11 GPa in a calcareous metapelite from the Dabie Mountains, China. Lithos 52:51–77.

Fasshauer DW, Chatterjee ND, Marler B (1997) Synthesis, structure, thermodynamic properties and stability relations of K–cymrite, $KAlSi_3O_8 \cdot H_2O$. Phys Chem Minerals 24:455–462.

Fasshauer DW, Wunder B, Chatterjee ND, Höhne GWH (1998) Heat capacity of wadeite–type $K_2Si_4O_9$ and the pressure–induced stable decomposition of K–feldspar. Contrib Mineral Petrol 131:210–218.

Faust J, Knittle E (1994) The equation of state, amorphization, and high–pressure phase diagram of muscovite. J Geophys Res 99:19,785–19,792.

Geisinger KL, Ross NL, McMillan P, Navrotsky A (1987) Potassium silicate ($K_2Si_4O_9$): energetics and vibrational spectra of glass, sheet silicate, and wadeite–type phases. Am Mineral 72:984–994.

Gillet P, Chen M, Dubrovinsky L, El Goresy A (2000) Natural $NaAlSi_3O_8$–hollandite in the shocked Sixiangkou meteorite. Science 287:1633–1636.

Harlow GE, Davies R (2004) Status report on stability of K–rich phases at upper–mantle conditions. Lithos 77:647–653.

Holland TJB (1989) Dependence of entropy on volume for silicate and oxide minerals: a review and a predictive model. Am Mineral 74:5–13.

Holland TJB, Powell R (1991) A compensated-Redlich-Kwong (CORK) equation for volumes and fugacities of CO_2 and H_2O in the range 1 bar to 50 kbar and 100 – 1600°C. Contrib MineralsPetrol 109:265–273.

Holland TJB, Powell R (1998) An internally consistent thermodynamic data set for phases of petrological interest. J Metam Geol 16:309–343.

Hwang SL, Shen P, Chu H-T, Yui T-F, Liou JG, Sobolev NV, Zhang R-Y, Shatsky VS, Zayachkovsky AA (2004) Kokchetavite: a new potassium-feldspar polymorph from the Kokchetav ultrahigh-pressure terrane. Contr Mineral Petrol 148:380–389.

Irifune T, Ringwood RE, Hibberson WO (1994) Subduction of continental crust and terrigenous and pelagic sediments: and experimental study. Earth Planet Sci Lett 126:351–368.

Kaneko Y, Maruyama S, Terabayashi M, Yamamoto H, Ishikawa M, Anma R, Parkinson CD, Ota T, Nakajima Y, Katayama I, Yamamoto J, Yamauchi K (2000) Geology of the Kokchetav UHP-HP metamorphic belt, Northern Kazakhstan. Island Arc 9:264-283.

Kimura M, Chen M, Yoshida Y, El Goresy A, Ohtani E (2004) Back–transformation of high–pressure phases in a shock melt vein of an H–chondrite during atmospheric passage: implications for the survival of high–pressure phases after decompression. Earth Planet Sci Lett 217:141–150.

Kinomura N, Koizumi M, Kume S (1977) Crystal structures of phases produced by disproportionation of K–feldspar under pressure. In: Manghnani MH, Akimoto S (eds) High–Pressure Research: Application in Geophysics. Academic Press, New York, pp 183–189.

Kinomura N, Kume N, Koizumi M (1975) Stability of $K_2Si_4O_9$ with wadeite type structure. Proc 4th Inter Conf High Pressure Sci Tech, pp 211–214.

Konzett J, Fei Y (2000) Transport and storage of potassium in the earth's upper mantle and transition zone: an experimental study to 23 GPa in simplified and natural bulk compostions. J Petrol 41:583–603.

Korsakov AV, Theunissen K, Smirnova LV (2004) Intergranular diamonds derived from partial melting of crustal rocks at ultrahigh-pressure metamorphic conditions. Terra Nova:146–151

Langenhorst F, Poirier JP (2000) "Eclogitic" minerals in a shocked basaltic meteorite. Earth Planet Sci Lett 176:259–265.

Liu L (1978) High–pressure phase transitions of kalsilite and related potassium bearing aluminosilicates. Geochemical Journal 12:275–277.

Massonne H-J (1992) Evidence for low-temperature ultrapotassic siliceous fluids in subduction zone environments from experiments in the system K2O-MgO-Al2O3-SiO2-H2O (KMASH). Lithos 28:421-434.

Massonne H-J (2003) Characterization of an early metamorphic stage through inclusions in zircon of a diamondiferous quartzofeldspathic rock from the Erzgebirge, Germany. Am Mineral 88:883–889

Ono S (1998) Stability limits of hydrous minerals in sediment and mid–ocean ridge basalt compositions: implications for water transport in subduction zones. J Geophys Res 103:18,253–18,267.

Prewitt CT, Downs RT (1998) High-pressure crystal chemistry. Rev Mineral 37: 283–312. **[Give title of Rev. and editors]**

Ringwood AE (1975) Composition and petrology of the Earth's mantle. McGraw-Hill, New York, pp 618.

Ringwood AE, Reid AF, Wadsley AD (1967) High–pressure $KAlSi_3O_8$, an alumino-silicate with sixfold coordination. Acta Crystallogr 23:1093–1095.

Robie RA, Hemingway BS (1995) Thermodynamic properties of minerals and related substances at 298.15 K and 1 bar (10^5 Pascals) pressure and at higher temperatures. US Geol Surv 2131, 461 pp 461

Schertl H-P, Schreyer w, Chopin C (1991) The pyrope-coesite rocks and their country rocks at Parigi, Dora Maira massif, western Alps: detailed petrography, mineral chemistry and PT-path. Contrib Mineral Petrol 108:1-21.

Schmidt M (1996) Experimental constraints on recycling of potassium from subducted oceanic crust. Science 272:1927–1930.

Schmidt MW, Poly S, Comodi P, Zanazzi PF (1997) High-pressure behavior of kyanite: Decomposition of kyanite into stishovite and corundum. Am Mineral 82:460–466

Seki Y, Kennedy GC (1964) The breakdown of potassium feldspar, $KAlSi_3O_8$, at high temperatures and high pressures. Am Mineral 49:1688–1706.

Sekine T, Rubin AM, Ahrens TJ (1991) Shock wave equation of state of muscovite. J Geophys Res 96:19,675–19,680.

Sharp ZD, Essene EJ, Hunziker JC (1993) Stable isotope geochemistry and phase equilibria of coesite-bearing whiteschists, Dora Maira massif, western Alps. Contrib Mineral Petrol 114:1-12.

Sueda Y, Irifune T, Nishiyama N, Rapp RP, Ferroir T, Onozawa T, Yagi T, Merkel S, Miyajima N, Funakoshi K (2004) A new high-pressure form of $KAlSi_3O_8$ under lower mantle conditions. Geophys Res Lett 31, L23612, doi:10.1029/2004GL021156.

Swanson DK, Prewitt CT (1983) The crystal structure of $K_2Si^{VI}–Si^{IV}_3O_9$. Am Mineral 68:581–585.

Swanson DK, Prewitt CT (1986) Anharmonic thermal motion in $K_2Si^{VI}–Si^{IV}_3O_9$. Eos 67:369.

Thompson P (1994) The sanidine-'sanidine hydrate' reaction boundary. Mineral Mag 58A:897.

Thompson P, Parsons I, Graham CM, Jackson B (1998) The breakdown of potassium feldspar at high water pressures. Contrib Min Petrol 130:176–186.

Tomioka N, Mori H, Fujino K (2000) Shock–induced transition of $NaAlSi_3O_8$ feldspar into a hollandite structure in a L6 chondrite. Geophys Res Lett 278:3997–4000.

Tutti F, Dubrovinsky LS, Saxena SK, Carlson S (2001) Stability of $KAlSi_3O_8$ hollandite-type structure in the Earth's lower mantle conditions. Geophys Res Lett 28:2735–2738.

Urakawa S, Kondo T, Igawa N, Shimomura O, Ohno H (1994) Synchrotron radiation study on the high-pressure and high-temperature phase relations of $KAlSi_3O_8$. Phys Chem Mineral 21:387–391.

Wang W, Takahashi E (1999) Subsolidus and melting experiments of a K-rich basaltic composition to 27 GPa: implication for the behavior of potassium in the mantle. Am Mineral 84:357–361.

Yagi A, Suzuki T, Akaogi M (1994) High pressure transitions in the system $KAlSi_3O_8$ –$NaAlSi_3O_8$. Phys Chem Minerals 21:12–17.

Yamada H, Matsui Y, Ito E (1984) Crystal–chemical characterization of $KAlSi_3O_8$ with hollandite structure. Mineral J 12:29–34.

Yoshida D, Hirajima T, Ishiwatari A (2004) Pressure-temperature path recorded in the Yangkou garnet peridotite, in Su-Lu ultrahigh-pressure metamorphic belt, eastern China. J Petrol 45:1125–1145.

Zhang J, Ko J, Hazen RM, Prewitt CT (1993) High–pressure crystal chemistry of $KAlSi_3O_8$ hollandite. Am Mineral 78:493–499.

Figure legends

Fig.1 Comparison of the low-T Cp of $KAlSi_3O_8$ hollandite measured using the PPMS calorimeter in this study with high-T Cp data from Akaogi et al. (2004)

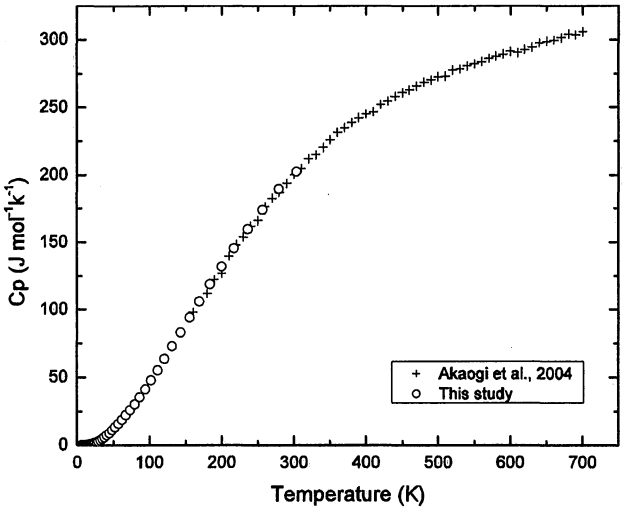

Fig. 2 Phase diagram for $KAlSi_3O_8$. *Dotted line* represents the coesite-stishovite transition boundary obtained with a modified Holland and Powell (1998) thermodynamic data base. *Dashed lines* show the phase boundaries calculated from $S^{o}_{298(Wd)}$=232 J $mol^{-1}K^{-1}$(Fasshauer et al., 1998). *Solid line* represents the phase boundaries calculated from $S^{o}_{298(Wd)}$=250.83 J $mol^{-1}K^{-1}$ and modified enthalpy of $KAlSi_3O_8$ hollandite. *Dash-dotted lines* are the phase boundaries of Akaogi et al. (2004). *Circles* represent quench experimental runs by Yagi et al. (1994) after pressure correction, and *squares* are the in situ X-ray experimental runs by Urakawa et al. (1994). *Open, closed* and *shaded symbols* represent hollandite, wadeite+kyanite+coesite (or stishovite), and sanidine, respectively. Hol hollandite; Wd wadeite; Ky kyanite; Coe coesite; Stv stishovite; San sanidine

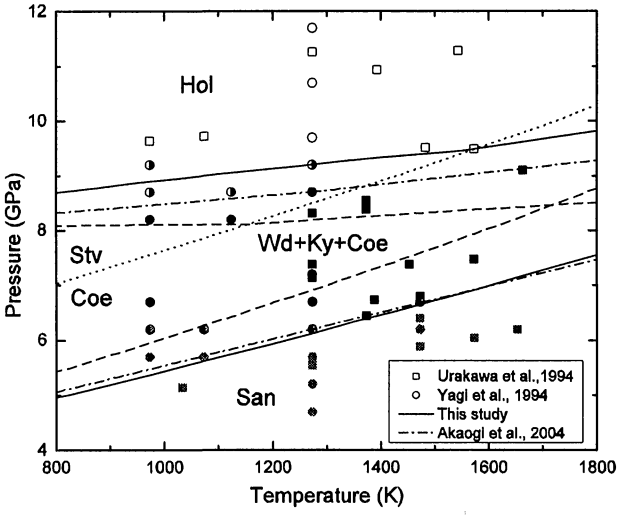

Fig. 3 Phase diagram in the system K_2O-Al_2O_3-SiO_2. Cor corundum; Ks kalsilite; Qz quartz; Lc leucite

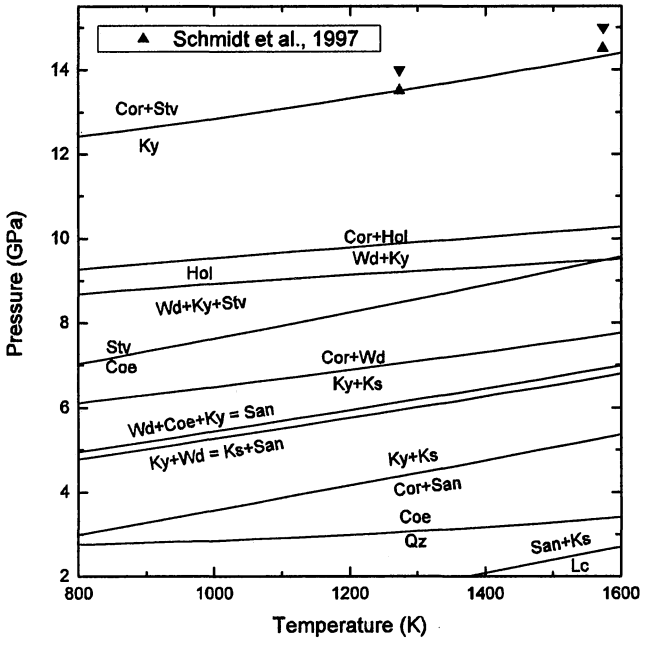

Fig. 4 Calculated P-T diagram for the formation of K-cymrite. The *open* and *closed triangles* represent the experimental reversals by Fasshauer et al. (1997) and Thompson et al. (1998), respectively. The *dashed line* represents the microline-sanidine transition boundary. Kcym K-cymrite; Mic microline

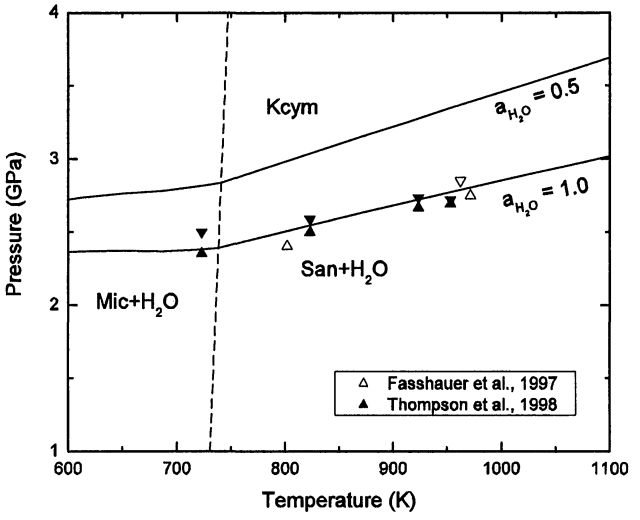

Fig. 5 Calculated P-T diagram for the dehydration reaction of K-cymrite into $KAlSi_3O_8$ hollandite. *Closed triangles* represent two experimental runs by Harlow and Davies (2004).

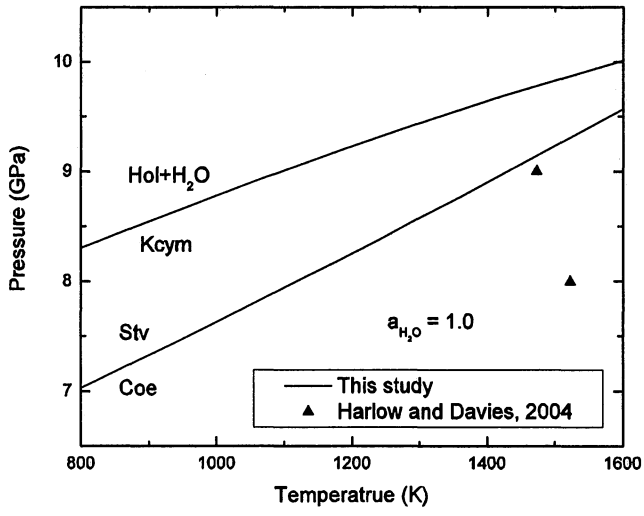

Fig. 6 Calculated P-T diagram for the dehydration reaction of muscovite into $KAlSi_3O_8$ hollandite + Al_2O_3 + H_2O. The *solid line* represents the calculated phase boundary in this study. The *dashed line* showes the calculated phase boundary by Sekine et al. (1991). Mu muscovite

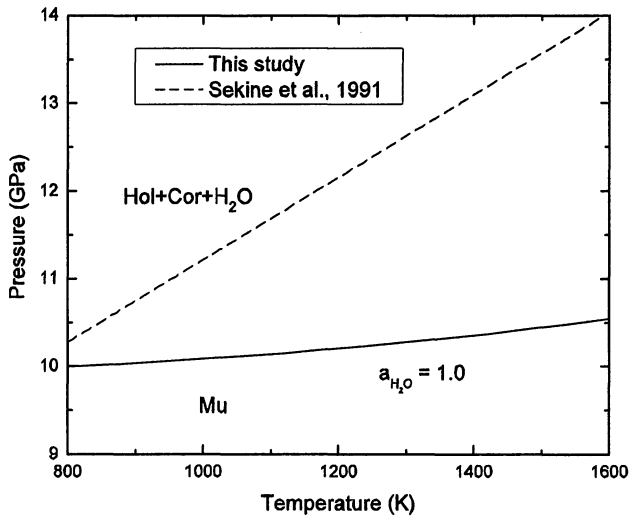

Table Title

Table 1 Composition of $KAlSi_3O_8$ hollandite used for heat capacity measurement

Phase	SiO_2	Al_2O_3	K_2O	MgO	Na_2O	FeO	Sum
$KAlSi_3O_8$ (hollandite)	65.35	17.28	16.52	0.04	0.03	0.05	99.56
Cations per 8 O	3.037	0.946	0.997	0.003	0.003	0.002	4.989

Table 2 Lattice parameters of $KAlSi_3O_8$ hollandite used for heat capacity measurement. The numbers in parentheses represent one standard deviation and they apply to the last digits of the preceding number.

Phase	a (Å)	b (Å)	c (Å)	α	β	γ	V (Å^3)	References
$KAlSi_3O_8$ (hollandite)	9.313(3)	9.313(3)	2.723(3)	90	90	90	236.22	This study
	9.3244(4)	9.3244(4)	2.7227(3)	90	90	90	236.73	Yamada et al. (1984)
	9.315(4)	9.315(4)	2.723(4)	90	90	90	236.26	Zhang et al. (1993)

Table 3 Measured heat capacity of $KAlSi_3O_8$ hollandite

T (K)	Cp (j $mol^{-1}K^{-1}$)	T (K)	Cp (j $mol^{-1}K^{-1}$)	T (K)	Cp (j $mol^{-1}K^{-1}$)
5.06	0.0177	20.87	1.059	86.45	35.52
5.52	0.0231	22.68	1.371	93.95	41.36
6.00	0.0305	24.65	1.792	102.17	47.91
6.52	0.0377	26.80	2.307	111.41	55.13
7.08	0.0494	29.14	2.986	120.78	63.77
7.69	0.0594	31.68	3.807	131.31	73.05
8.36	0.0776	34.45	4.810	142.77	83.25
9.08	0.0962	37.46	6.022	155.22	94.20
9.86	0.1232	40.74	7.484	168.72	106.16
10.72	0.1575	44.29	9.029	183.49	118.93
11.65	0.1947	48.15	11.00	199.47	132.06
12.67	0.2470	52.35	13.25	216.98	145.75
13.76	0.3096	56.92	15.87	235.83	159.92
14.96	0.3953	61.88	18.81	256.48	174.27
16.25	0.4997	67.28	22.16	278.71	189.62
17.67	0.6381	73.14	26.05	303.10	202.66
19.20	0.8188	79.52	30.30		

Table 4 Phase property data used for phase boundary calculation. The numbers in parentheses are 2 standard deviations.

Phase*	$H^\circ_{f,298}$	S°_{298}	$Cp=c_1+c_2T^{-0.5}+c_3T^{-2}+c_4T^{-3}$ (J mol^{-1}K^{-1})				V°_{298}	$\alpha=a_0+a_1T$ (K^{-1})		K_{0T}	K'_{0T}
	(kJ mol^{-1})	(J mol^{-1}K^{-1})	$c_1 \times 10^{-2}$	$c_2 \times 10^{-3}$	$c_3 \times 10^{-6}$	$c_4 \times 10^{-8}$	(cm^3 mol^{-1})	$a_0 \times 10^5$	$a_1 \times 10^8$	(Gpa)	
$KAlSi_3O_8$ (hol)	-3803.50[a]	166.2(0.4)[d]	3.896	-1.823	-12.934	16.307[f]	71.28[h]	3.300	0[f]	180[l]	4[n]
$K_2Si_4O_9$ (wd)	-4301.2(5.7)[b]	250.8(0.3)[e]	4.991	-4.350	0	0[b]	108.44[i]	2.950	0[j]	90[m]	4[n]
$KAlSi_3O_8 \cdot H_2O$(kcym)	-4238.00[c]	284.0[c]	4.812	-2.981	-9.931	14.165[g]	114.37[g]	1.816	2.129[k]	45.1[g]	1.3[g]

[a] Modified from Akaogi et al. (2004); [b] Fasshauer et al. (1998); [c] Modified from Fasshauer et al. (1997); [d] This study; [e] Estimated from Holland (1989); [f] Akaogi et al. (2004); [g] Fasshauer et al. (1997); [h] Yamada et al. (1984); [i] Swanson and Prewitt (1983); [j] Swanson and Prewitt (1986); [k] Calculated from Fasshauer et al. (1997); [l] Zhang et al. (1993); [m] Geisinger et al. (1987); [n] Assumed.

* All the other phases involved in this study are from a modified Holland and Powell (1998) data base, called hp02ver.dat. More detailed information about hp02ver.dat can be found in http://www.perplex.ethz.ch/.